ORGANOMETALLICS

Volume 7, Number 1, January 1988

Interaction of Trialkylaluminum Reagents with Metal-Bound Ethylene and Carbon Monoxide. The Molecular Structure of $(\eta^5\text{-}C_5Me_5)_2Ta(H)(C_2H_4{\cdot}AlEt_3)$

Christine McDade,[†] Vernon C. Gibson,[‡] Bernard D. Santarsiero, and John E. Bercaw*

Arthur Amos Noyes Laboratory of Chemical Physics,[§] California Institute of Technology, Pasadena, California 91125

Received January 22, 1987

The compounds $(\eta^5\text{-}C_5Me_5)_2M(H)(C_2H_4)$ and $(\eta^5\text{-}C_5Me_5)_2M(H)(CO)$ (M = Nb, Ta) reversibly bind trialkylaluminum reagents to give 1:1 adducts in which the aluminum is bonded to the metal-bound ethylene or carbonyl oxygen in preference to the hydride ligand. The mixed-ring compound $(\eta^5\text{-}C_5Me_5)(\eta^5\text{-}C_5H_5)Ta(H)(CO)$, in contrast, binds aluminum at the hydride ligand. The nature of the interactions has been established by IR and NMR studies and by determination of the molecular structure of $(\eta^5\text{-}C_5Me_5)_2Ta(H)(C_2H_4{\cdot}AlEt_3)$ at reduced temperature [$P2_1/c$, a = 14.877 (5) Å, b = 12.455 (7) Å, c = 15.017 (4) Å, β = 101.08 (13)°, V = 2730 (2) Å^3, T = 220 K, Z = 4, 2496 reflections, S (goodness-of-fit) = 2.75, 283 parameters, R = 0.054 (2033 reflections, $I > 3\sigma_I$)]. This structure displays an unusual ethylene bridge between the aluminum and tantalum centers. The significance of these adducts in the context of Ziegler–Natta catalysis and migratory insertion is discussed.

Introduction

Organoaluminum compounds are known to promote the stereoregular polymerization of olefins when combined with early-transition-metal complexes (Ziegler–Natta catalysis).[1–4] Despite the commercial importance of this process, little is known about the nature of the catalytic sites. It has generally been proposed that the organoaluminum compound both alkylates and reduces the transition-metal center and then coordinates to that metal center, primarily through halogen bridges.[1,5] The growing number of alkyl-bridged transition-metal–aluminum compounds[6–8] suggests that other alternatives are available.

The interaction of Lewis acids such as organoaluminum compounds with the oxygen atom of transition-metal–carbonyl–hydride compounds has been suggested to assist migratory insertion to the metal formyl, thus overcoming otherwise unfavorable thermodynamics for this step in the hydrogenation of carbon monoxide.[9] In fact, Shriver and co-workers have demonstrated tremendous rate accelerations for migratory insertion reactions of transition metal carbonyl alkyls in the presence of aluminum halides.[10] Attempts to observe similar rate accelerations for migratory insertion reactions of related transition-metal carbonyl hydrides were unsuccessful, however, when reaction with Lewis acids led to coordination at the hydride rather than the carbonyl oxygen.[11] Preference for Lewis acid coordination at a hydride instead of a carbonyl oxygen has also been observed by other workers.[12,13]

We have examined the reactivity of trialkylaluminum reagents with ethylene and carbonyl derivatives of permethylniobocene and permethyltantalocene, Cp^*_2M-

---

[†] Present address: Rohm and Haas Research Laboratories, 727 Norristown Road, Spring House, PA 19477.

[‡] Present address: Chemistry Department, University of Durham, South Road, Durham, DH1 3LE, U.K.

[§] Contribution No. 7383.

(1) Parshall, G. W. *Homogeneous Catalysis*; Wiley: New York, 1980.

(2) Ziegler, K. *Organometallic Chemistry*; Zeiss, H., Ed; Reinhold: New York, 1960; pp 194–195, 229–231.

(3) Mole, T.; Jeffrey, E. A. *Organoaluminum Compounds*; Elsevier: New York, 1972.

(4) Boor, J., Jr. *Ziegler-Natta Catalysis and Polymerization*; Academic: New York, 1979.

(5) Jonas, K.; Kruger, C. *Angew. Chem., Int. Ed. Engl.* **1980**, *19*, 520.

(6) Holton, J.; Lappert, M. F.; Ballard, D. G. H.; Pierce, R.; Atwood, J. L.; Hunter, W. E. *J. Chem. Soc., Dalton Trans.* **1979**, 45–53.

(7) Scollary, G. R. *Aust. J. Chem.* **1978**, *31*, 411–414.

(8) Wilke, G. Presented at the 23rd International Conference on Coordination Chemistry, Boulder, CO; July 29-Aug 3, 1984.

(9) Wolczanski, P. T.; Bercaw, J. E. *Acc. Chem. Res.* **1980**, *13*, 121–127.

(10) Butts, S. B.; Straus, S. H.; Holt, E. M.; Stimson, R. E.; Alcock, N. W.; Shriver, D. F. *J. Am. Chem. Soc.* **1980**, *102*, 5093–5100.

(11) Richmond, T. G.; Basolo, F.; Shriver, D. F. *Organometallics* **1982**, *1*, 1624–1628.

(12) (a) Tebbe, F. N. *J. Am. Chem. Soc.* **1973**, *95*, 5412–5414. (b) Otto, E. H.; Brintzinger, H. H. *J. Organomet. Chem.* **1979**, *170*, 209–216.

(13) Examples of M–H–Al bridges in compounds not containing carbonyls also exist: (a) Bruno, J. W.; Huffman, J. C.; Caulton, K. G. *J. Am. Chem. Soc.* **1984**, *106*, 444–445. (b) Wailes, P. C.; Weigold, H.; Bell, A. P. *J. Organomet. Chem.* **1972**, *43*, 29–31. (c) Lobkovskii, E. B.; Soloreichik, G. L.; Sisov, A. I.; Bulychev, B. M.; Gusev, A. I.; Kirillova, N. I. *J. Organomet. Chem.* **1984**, *265*, 167–173.

0276-7333/88/2307-0001$01.50/0 © 1988 American Chemical Society

$(H)(C_2H_4)$ ($Cp^* = \eta^5\text{-}C_5Me_5$; M = Nb (**1**); M = Ta (**2**)) and $Cp^*_2M(H)(CO)$ (M = Nb (**3**); M = Ta (**4**)) and the mixed-ring complex $Cp^*CpTa(H)(CO)$ ($Cp = \eta^5\text{-}C_5H_5$ (**5**)). Tebbe has shown that the parent compounds $Cp_2Nb(H)(C_2H_4)$ and $Cp_2Nb(H)(CO)$ react with trialkylaluminum reagents at the hydride ligand in each case, inhibiting the known insertion of ethylene into the Nb–H bond.[12a] Due to the larger steric bulk of the permethylcyclopentadienyl ligands, we anticipated the M–H bond might be shielded from the trialkylaluminum reagent, encouraging interaction with the ethylene or carbonyl ligands. Compounds **1** and **2** undergo reversible insertion of the coordinated ethylene into the metal–hydride bond, the first step in a postulated mechanism of the polymerization process,[14] at rates that are conveniently measured by ^1H NMR techniques.[15] Compounds **3**, **4**, and **5**, however, show no propensity to form formyl complexes under a variety of conditions. The nature of the interactions of trialkylaluminum compounds with **1–5** and the effect of the added trialkylaluminum reagent on the rate of possible insertion reactions were consequently of some interest.

Results and Discussion

Addition of equimolar amounts of $AlMe_3$ or $AlEt_3$ to a petroleum ether solution of **1**, **2**, **3**, or **4** yields 1:1 adducts that are air, moisture, and thermally sensitive solids (eq 1 and 2). They may be isolated in excellent yields at −80 °C as pale yellow (**6** and **7**) or bright blue (**8** and **9**) microcrystals. Each has been characterized by NMR and IR spectroscopies and, for the niobium compounds, microanalysis.

$$\begin{array}{lll} Cp^*_2M(H)(C_2H_4) + AlR_3 & \rightarrow Cp^*_2M(H)(C_2H_4{\cdot}AlR_3) & (1) \\ \quad \mathbf{1}\text{: } M = Nb & \quad \mathbf{6a}\text{: } M = Nb, R = Me & \\ \quad \mathbf{2}\text{: } M = Ta & \quad \mathbf{6b}\text{: } M = Nb, R = Et & \\ & \quad \mathbf{7}\text{: } M = Ta, R = Et & \end{array}$$

$$\begin{array}{lll} Cp^*_2M(H)(CO) + AlR_3 & \rightarrow Cp^*_2M(H)(CO{\cdot}AlR_3) & (2) \\ \quad \mathbf{3}\text{: } M = Nb & \quad \mathbf{8a}\text{: } M = Nb, R = Me & \\ \quad \mathbf{4}\text{: } M = Ta & \quad \mathbf{8b}\text{: } M = Nb, R = Et & \\ & \quad \mathbf{9}\text{: } M = Ta, R = Et & \end{array}$$

In contrast to the above compounds, where the aluminum reagent coordinates to an ethylene or carbonyl ligand (vide infra), the aluminum adduct of **5**, in which one of the Cp* ligands has been replaced by a less sterically demanding Cp ligand, forms at the hydride (eq 3). Compound **10** has also been characterized by NMR and IR spectroscopies.

$$\underset{\mathbf{5}}{Cp^*CpTa(H)(CO)} + AlEt_3 \rightarrow \underset{\mathbf{10}}{Cp^*CpTa(H{\cdot}AlR_3)(CO)} \quad (3)$$

Spectroscopic data for compounds **6–10** are very dependent on temperature and on concentration of the aluminum reagent (e.g., see Figure 1). This dependence suggests a dynamic equilibrium between the reagents and the 1:1 adducts (eq 4 and 5). Similar equilibria have been noted in other aluminum/transition-metal systems.[16,17]

$$Cp^*_2M(H)(Y) + AlR_3 \rightleftharpoons Cp^*_2M(H)(Y{\cdot}AlR_3) \quad (4)$$

$$M = Nb, Ta;\ Y = C_2H_4, CO;\ R = Me, Et$$

$$Cp^*CpTa(H)(CO) + AlEt_3 \rightleftharpoons Cp^*CpTa(H{\cdot}AlEt_3)(CO) \quad (5)$$

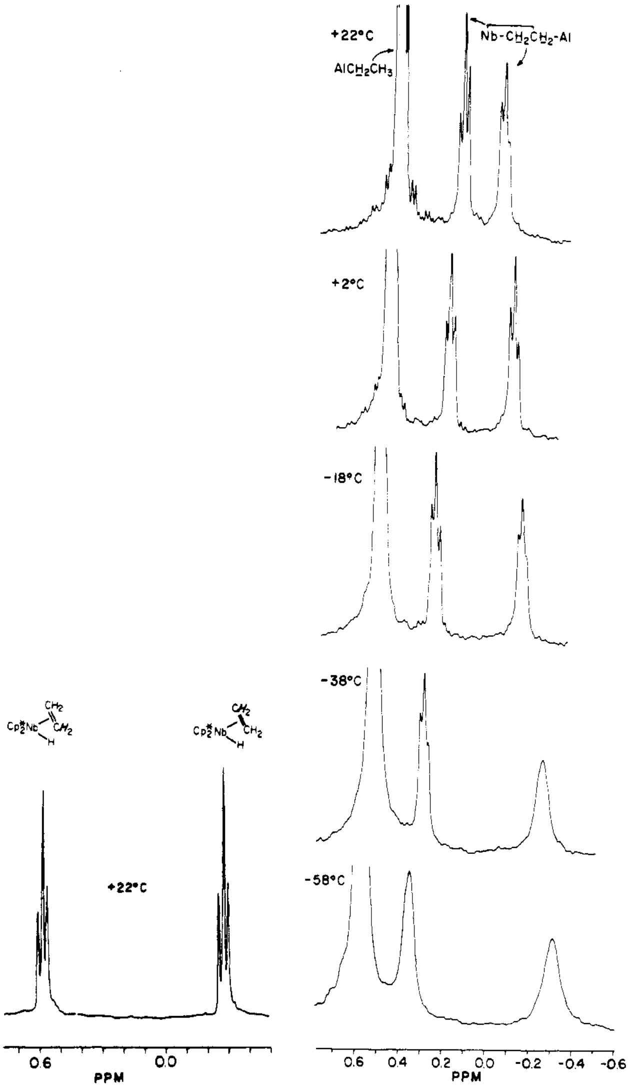

Figure 1. Variable-temperature ^1H NMR (500.13 MHz) spectra for a solution of **1** and 1.06 equiv of $AlEt_3$ (right). A portion of the ^1H NMR (500.13 MHz) spectrum for **1** at 22 °C is shown for comparison (left). Solvent: toluene-d_8.

The coordination of the organoaluminum compound at the ethylene or carbonyl ligand in **6–9** and not at the hydride is unexpected on the basis of literature precedent. While coordination of aluminum compounds at metal carbonyls has been observed in many cases,[11,18] it has never been reported when a hydride or halide ligand was also present.[19] To our knowledge, coordination of an aluminum compound at a metal-bound ethylene has not been

---

[14] (a) Evitt, E. R.; Bergman, R. G. *J. Am. Chem. Soc.* **1980**, *102*, 7003–7011. (b) Schmidt, G. F.; Brookhart, M. *Ibid.* **1985**, *107*, 1443–1444.

[15] (a) Doherty, N. M.; Bercaw, J. E. *J. Am. Chem. Soc.* **1985**, *107*, 2670–2682. (b) Doherty, N. M. *Ph.D.* Thesis, California Institute of Technology, 1984. (c) Burger, B. J.; Bercaw, J. E., unpublished results.

[16] (a) Kotz, J. C.; Turnipseed, C. D. *J. Chem. Soc., Chem. Commun.* **1970**, 41–42. (b) Burlitch, J. M.; Leonowics, M. E.; Peterson, R. B.; Hughes, R. E. *Inorg. Chem.* **1979**, *18*, 1097–1105. (c) Mayer, J. M.; Calabrese, J. C. *Organometallics* **1984**, *3*, 1292–1298.

[17] These ν(NbH) bands for $Cp^*_2NbH_3$ and $Cp^*_2NbH_2(H{\cdot}AlEt_3)$ are rather broad and unresolved. It is likely that the ν(NbH) band for $Cp^*_2NbH_2(H{\cdot}AlEt_3)$ includes contributions from the uncomplexed terminal hydrides. Also, because of the high coupling of IR bands within the molecules, it is not possible to clearly assign bands for the ethylene ligand in compounds **1** and **2** or **6** and **7**. Full IR data are reported in: McDade, C. Ph.D. Thesis, California Institute of Technology, 1985.

[18] (a) The first C- and O-bonded carbon monoxide, at a bridging carbonyl group, was reported by Shriver and co-workers in the previous year: Nelson, N. J.; Kime, N. E.; Shriver, D. F. *J. Am. Chem. Soc.* **1969**, *91*, 5173–5174. (b) Kotz and Turnipseed provided the first example of Lewis basicity at a terminal carbonyl's oxygen.[16a] (c) Shriver, D. F.; Alich, A. *Coord. Chem. Rev.* **1972**, *8*, 15–20. (d) Butts, S. B.; Straus, S. H.; Holt, E. M.; Stimson, R. E.; Alcock, N. W.; Shriver, D. F. *J. Am. Chem. Soc.* **1980**, *102*, 5093–5100. (e) Lindner, E.; von Au, E. *Angew. Chem., Int. Ed. Engl.* **1980**, *19*, 824–825.

[19] (a) Pankowski, M.; Demerseman, B.; Bouquet, G.; Bigorgne, M. *J. Organomet. Chem.* **1972**, *35*, 155–159. (b) Powell, P.; Noth, H. *J. Chem. Soc., Chem. Commun.* **1966**, 637–638. (c) Otto, E. H.; Brintzinger, H. H. *J. Organomet. Chem.* **1979**, *170*, 209–216.

reported either,[20] although saturated alkyl-bridged transition-metal–aluminum compounds are known.[6-8] That the transition-metal–aluminum complexes obtained in these studies are indeed carbonyl- and ethylene-bound or hydride-bound is supported by examination and comparison of the spectroscopic characteristics of compounds **6**–**10** with those of previously reported compounds. Additionally, the molecular structure of **7** has been determined by single-crystal X-ray diffraction.

The positions of the IR bands for ν(M–H) and ν(CO) change markedly upon complexation of the trialkylaluminum reagent. The IR band for ν(Nb–H) shifts from 1710 cm^{-1} in **1** to 1769 cm^{-1} in **6a** and 1760 cm^{-1} in **6b** and ν(Ta–H) from 1765 cm^{-1} in **2** to 1850 cm^{-1} in **7**. Tebbe did not report the infrared spectra of $Cp_2Nb(C_2H_4)(H{\cdot}AlEt_3)$ and $Cp_2NbH_2(H{\cdot}AlEt_3)$,[12a] but coordination of $AlEt_3$ to the central hydride of $Cp^*{}_2NbH_3$ results in a decrease in ν(Nb–H) from 1752 to 1736 cm^{-1}.[17] Coordination of $AlEt_3$ to **5** resulted in a decrease in ν(Ta–H) from 1740 to 1725 cm^{-1} in **10**.

More data are available from the infrared spectra of the carbonyl–aluminum complexes. The band for ν(CO) decreases from 1875 cm^{-1} in **3** to 1721 cm^{-1} in **8a** or 1737 cm^{-1} in **8b** and from 1865 cm^{-1} in **4** to 1725 cm^{-1} in **9**. Similar decreases in ν(CO) with Lewis acid complexation are observed for $Cp^*{}_2Nb(R)(CO)$ (R = CH_3, CH_2CH_3, CH_2CH_2Ph, $C(CH_3){=}CH(CH_3)$)[17] and for other transition metal–carbonyl compounds without hydrides reported previously.[11,18] The opposite result, a moderate increase in ν(CO), is taken as primary evidence against CO coordination of aluminum in hydride- or halide-containing transition-metal compounds[16bc,19,21] and was also observed in the mixed-ring compound $Cp^*CpTa(H{\cdot}AlEt_3)(CO)$ (1863 cm^{-1} for the uncomplexed species **5** vs 1900 cm^{-1} for the complexed species **10**). While Tebbe did not report the infrared spectrum of $Cp_2Nb(H{\cdot}AlEt_3)(CO)$, he did remark there was no significant shift in ν(CO) on its formation.[12a]

The ^1H NMR spectra of **6** and **7** all show small downfield shifts of the MH resonance (δ −2.73 (**6a**), −2.40 (**6b**), −1.65 (**7**)) relative to the position of that resonance in **1** (δ −3.04) and **2** (δ −2.84). The direction and magnitude of this shift contrast with the large upfield shift observed for $Cp_2Nb(C_2H_4)(H{\cdot}AlEt_3)$ (δ −9.63) relative to its precursor $Cp_2Nb(C_2H_4)(H)$ (δ 2.95).[12a] The small *downfield* shifts for the metal–hydride resonances of **6** and **7** are also found in **8** and **9** (δ −5.59 (**3**) vs δ −4.72 (**8a**) and δ −4.77 (**8b**); δ −5.15 (**4**) vs δ −3.18 (**9**)), which again contrast with data from the parent system, where the NbH resonance for $Cp_2Nb(H{\cdot}AlEt_3)(CO)$ is 5.1 ppm *upfield* of the same resonance for $Cp_2Nb(H)(CO)$.[12a,22a] A very large upfield shift of the hydride resonance is also found on formation of $Cp^*CpTa(H{\cdot}AlEt_3)(CO)$ (**10**) from $Cp^*CpTa(H)(CO)$ (**5**) (δ −10.2 and −5.48, respectively).[22b]

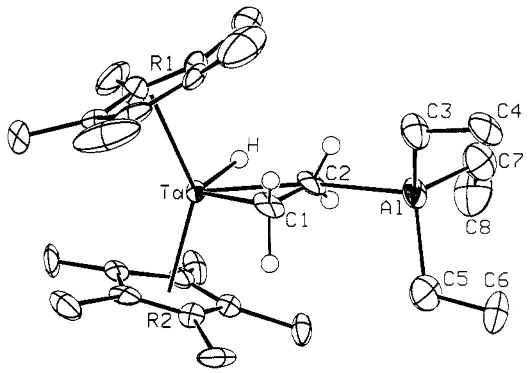

Figure 2. ORTEP diagram of $Cp^*{}_2Ta(H)(C_2H_4{\cdot}AlEt_3)$ (**7**). Crystal data: $C_{28}H_{50}AlTa$; M_r 594.63; monoclinic; space group $P2_1/c$; a = 14.877 (5) Å, b = 12.455 (7) Å, c = 15.017 (4) Å; β = 101.08 (13)°; V = 2730 (2) Å^3; Z = 4; T = 220 K.

The steric bulk of the Cp* ligands appears to be the factor controlling the site of the aluminum coordination. Even the replacement of a single Cp* ligand by Cp in **5** is sufficient to allow the trialkylaluminum reagent to coordinate at the hydride ligand and not at the carbonyl in **10**. Steric factors are known to dominate the formation and stability of aluminum dimers and donor–acceptor complexes,[3] and the formation constants for **6b**, **8a**, and **8b** give additional evidence of their importance in these compounds. The formation constant for adduct **6b** (K_{Et}, eq 7) in benzene solution at room temperature, determined from changes in the position and intensity of ν(Nb–H) (vide supra) with changes in [$AlEt_3$], is 2.4 (6) × 10^2 M^{-1}. The formation constants for **8a** and **8b** (K_{CO}, eq 8), determined similarly from changes in the position and intensity of ν(CO) with changes in [AlR_3], are 1.1 (2) × 10^5 and 4.5 (3) × 10^3 M^{-1}, respectively.

$$(AlR_3)_2 \overset{K_{Al}}{\rightleftharpoons} 2AlR_3 \qquad (6)$$

$$\underset{\mathbf{1}}{Cp^*{}_2Nb(H)(C_2H_4)} + AlEt_3 \overset{K_{Et}}{\rightleftharpoons} \underset{\mathbf{6b}}{Cp^*{}_2Nb(H)(C_2H_4{\cdot}AlEt_3)} \qquad (7)$$

$$\underset{\mathbf{3}}{Cp^*{}_2Nb(H)(CO)} + AlR_3 \overset{K_{CO}}{\rightleftharpoons} \underset{\substack{\mathbf{8a}:\ R\,=\,Me \\ \mathbf{8b}:\ R\,=\,Et}}{Cp^*{}_2Nb(H)(CO{\cdot}AlR_3)} \qquad (8)$$

The Nb–ethylene–Al adduct **6b** is the least stable with respect to equilibrium with its components, probably due to the less basic site of coordination, the ethylene ligand, available to the aluminum reagent. The Nb–carbonyl–triethylaluminum compound **8b** is less stable than the trimethylaluminum adduct **8a**. The lower formation constant for **8b** relative to **8a** is probably due to the greater steric interactions between the pentamethylcyclopentadienyl ligands on Nb and the alkyl groups on aluminum. Overall, however, **8b** is formed in similar quantity to **8a** under identical conditions ($K_{Al}K_{CO}$ = 0.99 × 10^{-2} and 1.0 × 10^{-2}, respectively) because the monomer–dimer equilibria of the trialkylaluminum reagents (eq 6) lies much more on the side of the dimer for $AlMe_3$ than for $AlEt_3$, negating the higher formation constant of **8a**.

The X-ray crystal structure of compound **7** was determined to verify the postulate that aluminum was indeed coordinated to the ethylene ligand and to examine the details of this unusual mode of bonding. The structure had to be obtained at low temperature (T = 220 K) due to the thermal instability of the complex when kept for long periods above −30 °C. Loss of the trialkylaluminum occurs above this temperature as the equilibrium analogous to eq 7 becomes significant and **7** decomposes to **2** in the absence of excess $AlEt_3$. This decomposition is even more rapid above −30 °C in the niobium analogue **6b**, which prevented us from obtaining the structure of **6b**. An ORTEP

---

(20) Kaminsky and co-workers have obtained the molecular structures of some zirconium compounds in which the linkage $ZrCH_2CH(AlEt_2)_2$ is present. Kaminsky, W.; Kopf, J.; Sinn, H.; Vollmer, H.-J. *Angew. Chem., Int. Ed. Engl.* **1976**, *15*, 629–630.

(21) Karlin, K. D.; Johnson, B. F. G.; Lewis, J. *J. Organomet. Chem.* **1978**, *160*, C21–C23.

(22) (a) $Cp^*{}_2NbH_2(H{\cdot}AlEt_3)$ exhibits both a small downfield shift of the resonance for the two outer Nb–H bonds and a larger upfield shift of the resonance for the central Hb–H bond,[17] as did $Cp_2TaH_2(H{\cdot}AlEt_3)$.[12a] (b) The complete NMR spectra of compounds **1**,[15a] **3**,[30] and **2**, **4**, and **5**[31] have previously been reported. The negative signs for the TaH resonances in the proton NMR spectra of **4** and **5** were inadvertently omitted in ref 31, however, and are corrected here.

Table I. Selected Bond Lengths (Å) and Angles (deg)

Ta–R(1)	2.130		
Ta–R(2)	2.120	R(1)–Ta–R(2)	138.9
Ta–C(1)	2.18 (2)	C(1)–Ta–C(2)	37.4 (6)
Ta–C(2)	2.31 (2)	Ta–C(1)–C(2)	76.0 (10)
C(1)–C(2)	1.44 (3)	Ta–C(2)–C(1)	66.6 (10)
Al–C(2)	2.25 (2)	Ta–C(2)–Al	163.8 (9)
Al–C(3)	1.98 (2)	C(2)–Al–C(3)	108.0 (7)
Al–C(5)	1.99 (2)	C(2)–Al–C(5)	105.8 (7)
Al–C(7)	1.97 (2)	C(2)–Al–C(7)	102.9 (7)
C(1)–H(11)	1.16 (15)	C(1)–C(2)–Al	97.8 (11)
C(1)–H(12)	0.82 (16)	H(11)–C(1)–H(12)	114 (13)
C(2)–H(21)	0.91 (15)		
C(2)–H(22)	0.83 (16)	H(21)–C(2)–H(22)	97 (15)
Ta–H	1.77	H–Ta–C(2)	72.6
Ta–C(2)–C(1)–H(11)	102 (8)	Ta–C(2)–C(1)–H(12)	-121 (12)
Ta–C(1)–C(2)–H(21)	-76 (15)	Ta–C(1)–C(2)–H(22)	111 (13)
Al–C(2)–C(1)–H(11)	-73 (8)	Al–C(2)–C(1)–H(12)	63 (12)
Ta–C(11)	2.43 (2)	C(15)–C(11)–C(12)	109.5 (14)
Ta–C(12)	2.41 (2)	C(11)–C(12)–C(13)	106.4 (14)
Ta–C(13)	2.45 (2)	C(12)–C(13)–C(14)	108.9 (14)
Ta–C(14)	2.43 (2)	C(13)–C(14)–C(15)	107.5 (15)
Ta–C(15)	2.49 (2)	C(14)–C(15)–C(11)	107.4 (14)
Ta–C(21)	2.47 (2)	C(25)–C(21)–C(22)	105.8 (13)
Ta–C(22)	2.44 (2)	C(21)–C(22)–C(23)	108.5 (13)
Ta–C(23)	2.43 (2)	C(22)–C(23)–C(24)	107.8 (14)
Ta–C(24)	2.43 (2)	C(23)–C(24)–C(25)	109.6 (14)
Ta–C(25)	2.45 (2)	C(24)–C(25)–C(21)	108.3 (13)
C(11)–C(11M)	1.47 (2)	C(15)–C(11)–C(11M)	124.5 (15)
C(12)–C(12M)	1.48 (2)	C(11)–C(12)–C(12M)	125.1 (14)
C(13)–C(13M)	1.52 (3)	C(12)–C(13)–C(13M)	124.3 (15)
C(14)–C(14M)	1.53 (3)	C(13)–C(14)–C(14M)	125.2 (17)
C(15)–C(15M)	1.49 (3)	C(14)–C(15)–C(15M)	123.7 (16)
C(21)–C(21M)	1.48 (2)	C(25)–C(21)–C(21M)	124.1 (14)
C(22)–C(22M)	1.50 (2)	C(21)–C(22)–C(22M)	123.8 (14)
C(23)–C(23M)	1.52 (2)	C(22)–C(23)–C(23M)	123.2 (14)
C(24)–C(24M)	1.49 (2)	C(23)–C(24)–C(24M)	124.8 (14)
C(25)–C(25M)	1.50 (2)	C(24)–C(25)–C(25M)	128.2 (14)

Table II. Least-Squares (Cp*) Planes

ring atoms[a]	Δ[b]	methyl atoms	Δ[b]
C(11)	-0.010	C(11M)	0.173
C(12)	-0.011	C(12M)	0.149
C(13)	0.029	C(13M)	0.348
C(14)	-0.035	C(14M)	0.055
C(15)	0.027	C(15M)	0.297
C(21)	0.004	C(21M)	0.328
C(22)	-0.014	C(22M)	0.164
C(23)	0.003	C(23M)	0.192
C(24)	-0.001	C(24M)	0.307
C(25)	-0.002	C(25M)	0.195

[a] The five inner-ring carbon atoms are included in the definition of the least-squares plane. [b] Displacement from the least-squares plane (Å).

diagram of the structure of 7 is given in Figure 2, and the structural features are summarized in Tables I and II.

The environment about the Ta center shows η^5 coordination of the two Cp* ligands, with an average Ta–C bond length of 2.44 Å, η^2 coordination of the ethylene, with Ta–C(1) = 2.18 (2) Å and Ta–C(2) = 2.31 (2) Å, and a Ta–H bond of approximately 1.8 Å.[23] The triethylaluminum ligand is bonded to carbon atom C(2), with the aluminum atom lying roughly in the Ta–C(1)–C(2) plane (displacement 0.18 Å). The hydrogen atoms on both methylene units were clearly resolved on difference Fourier maps and were refined with the other atoms.

Thus, the structure of 7 is of a previously unknown type, with ethylene bridging a transistion metal and a main-group metal. The following features are notable in this structure: (1) the Al–C(2) bond, at 2.25 (2) Å, is significantly longer than the Al–C(Et) bonds, which average 1.981 Å; (2) the Ta(C(2) bond is longer than the Ta–C(1) bond (Table I); (3) the C(1)–C(2) bond length is 1.44 (3) Å, intermediate between that of a single and a double C–C bond; and (4) the CH_2 plane on C(2) is tipped toward the Al atom, with both H(21) and H(22) canted toward the Al atom.[24] If H′ is defined as the midpoint between H(21) and H(22), the Ta–C(2)–H′ angle is 119° and the Al–C(2)–H′ angle is 77°.[25] Thus, the geometry about C(2) is like that of an S_E2 transition state for the incipient zwitterion $[Cp^*_2Ta^+H(CH_2CH_2Al^-Et_3)]$.

The effect of coordinated aluminum on the rate of insertion of ethylene or CO into a M–H bond has been probed by dynamic ^1H NMR studies on **6b** and its precursor 1 and by standard ^1H studies on **8b** and its precursor 3. For 1, a three-proton exchange process is observed between the two endo-hydrogen atoms (H) and the metal hydride, indicative of a reversible olefin insertion/β-H elimination (eq 9).[15,26] The same averaging process is

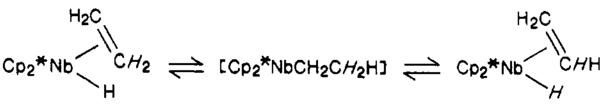

(9)

observed for **6b**, but a higher temperature (120 °C) is required to collapse the hydride and the endo-hydrogen signals even though the separation of these signals is less than that for 1. Although a quantitative rate of exchange should be accessible through magnetization transfer techniques, qualitative results are adequate for our purpose here. Clearly, coordination of $AlEt_3$ to the endo carbon *slows down* the migratory hydride insertion process for **6b**. This rate depression suggests that such interactions are not likely to accelerate olefin insertion processes in Ziegler–Natta polymerization.[12a,27]

Similarly, the addition of trialkylaluminum reagents to hydride–carbonyl complexes 8 and 9 did not result in CO insertion. Formation of a transition-metal–formyl complex from the hydride carbonyls 3 and 4 is not known in the absence of AlR_3, and it is not found in the presence of the trialkylaluminums or $AlBr_3$.[17] The alkyl–carbonyl compounds 11–14 were also examined for the effect of AlR_3 on CO insertion (alkyl migration). Compounds 11–14 *are* known to insert CO into the Nb–C bond when heated with excess carbon monoxide.[15b] It might be expected that the presence of equilibrium amounts of uncomplexed niobium–alkyl–carbonyl compounds, similar to the uncomplexed niobium–hydride–carbonyl compounds observed in solutions of 8, would influence the reactivity of compounds 11–14. However, these compounds behave quite differently from their precursors. Compounds 11, 12, and

---

[23] The hydride atom could not be refined but was resolved on a difference Fourier map.

[24] Conformational analysis of the structure using CHEMGRAF (Exxon Corporate Research) was undertaken to evaluate the importance of steric interactions on the structure of the transition metal–ethylene–aluminum adduct. Variations from the observed disposition of $AlEt_3$ relative to C_2H_4 are less favorable. The crystal structure is at a minimum in the van der Waals contact energy between the Al ethyls and the Ta ligands, but the potential well is fairly shallow over about 50° of rotation of $AlEt_3$ about an axis through the endo C of the ethylene unit and perpendicular to it. However, the potential wall rises sharply if the triethylaluminum is moved very much toward a more symmetrical position with respect to the ethylene.

[25] For comparison, the Ta–C(1–)–H″ angle of 135° is approximately equal to the C(2)–C(1)–H″ angle of 140°, with H″ defined as the midpoint between H(11) and H(12).

[26] $Cp^*_2Nb(H)(C_2H_4)$ (1) displays an AA′BB′X pattern for the olefin and hydride sites. As the temperature is raised, the hydride resonance and the signal due to the endo hydrogens broaden and collapse into the base line (at 90 °C) while the resonance of the exo hydrogens resolves into a pseudoquartet (J = 7 Hz).[15a]

[27] It is likely that dissociation of $AlEt_3$ precedes the migration of hydride. We have not examined the effect of the $[AlEt_3]$ on the coalescence temperature, however.

13a are, unlike their uncomplexed analogues, unstable in solution at room temperature. They decompose by transalkylation, via an as yet undetermined mechanism, followed by β-hydrogen elimination to produce ethylene (eq 10–12). Compound **13b** also transalkylates (eq 13); it

$$\underset{\mathbf{11}}{\mathrm{Cp^*_2Nb(Me)(CO{\cdot}AlEt_3)}} \rightarrow \mathrm{Cp^*_2Nb(Et)(CO{\cdot}AlMeEt_2)} \qquad (10)$$

$$\mathrm{Cp^*_2Nb(Et)CO{\cdot}AlREt_2)} \rightarrow \mathrm{Cp^*_2Nb(H)(CO{\cdot}AlREt_2)} + \mathrm{C_2H_4} \qquad (11)$$

$$\mathrm{R = Me,\ Et\ (12),\ CH_2CH_2Ph}$$

$$\underset{\mathbf{13a}}{\mathrm{Cp^*_2Nb(CH_2CH_2Ph)(CO{\cdot}AlEt_3)}} \rightarrow \mathrm{Cp^*_2Nb(Et)(CO{\cdot}AlEt_2CH_2CH_2Ph)} \qquad (12)$$

$$\underset{\mathbf{13b}}{\mathrm{Cp^*_2Nb(CH_2CH_2Ph)(CO{\cdot}AlMe_3)}} \rightarrow \underset{\mathbf{15}}{\mathrm{Cp^*_2Nb(Me)(CO{\cdot}AlMe_2CH_2CH_2Ph)}} \qquad (13)$$

$$\underset{\mathbf{14}}{\mathrm{Cp^*_2Nb(C(Me){=}C(Me)H)(CO{\cdot}AlEt_3)}} + \mathrm{CO} \rightarrow \underset{\mathbf{16}}{\mathrm{Cp^*_2Nb(C(Me){=}C(Me)H)(CO)}} \qquad (14)$$

forms a niobium–methyl compound. Since this new compound does not contain a β-hydrogen, the elimination step is not observed and a single clean product is produced by the first-order transalkylation. Compound **14** (eq 14) is different from **11–13**, for it is stable for weeks in solution while its uncomplexed precursor **16** loses CO over days in room temperature solutions not maintained in the dark, producing $\mathrm{Cp^*_2Nb(2\text{-}butyne)(H)}$. The precursor **16** can be heated (120 °C) in the presence of CO to produce an inserted product $\mathrm{Cp^*_2Nb(C({=}O)C(Me){=}C(Me)H(CO)}$,[15b] but when **14** is handled under identical conditions (eq 14), the only niobium product (^{1}H NMR) is $\mathrm{Cp^*_2Nb(C(Me){=}C(Me)H)(CO)}$ (**16**). Free ethane and ethylene are also observed, and no peaks assignable to $\mathrm{AlEt_3}$ are found.

Conclusion

We have isolated and examined the structure and reactivity of trialkylaluminum adducts of pentamethylcyclopentadienylniobium and -tantalum compounds. The trialkylaluminum adducts of ethylene–hydride compounds have aluminum coordinated at one carbon of the ethylene unit, while those of hydride–carbonyl and alkyl–carbonyl compounds have aluminum coordinated at the carbonyl oxygen. Only the mixed-ring tantalum hydride–carbonyl compound formed an aluminum complex at the hydride. While transition-metal–carbonyl–aluminum compounds have been described in the literature, the coordination of a Lewis acid to a carbonyl oxygen in preference to a metal hydride has not, to our knowledge, been previously reported. In these systems, only the presence of two pentamethylcyclopentadienyl ligands allows coordination at a ligand other than hydride. Significantly, the coordination of trialkylaluminum to the carbonyl oxygen does *not* appear to encourage carbonyl insertion reactions. Similarly, the coordination of trialkylaluminum to the ethylene ligand, a previously unreported type of compound whose structure resembles that of an S_E2 transition state, *slows* the rate of ethylene insertion into the metal–hydride bond and, by extension, likely does *not* facilitate Ziegler–Natta polymerization.

Experimental Section

General Considerations. All manipulations were performed by using glovebox or high vacuum line techniques. Solvents were dried over $\mathrm{LiAlH_4}$ or Na/benzophenone and stored under vacuum over "titanocene".[28] The NMR solvents, benzene-d_6 and toluene-d_8, were dried over activated molecular sieves (4 Å, Linde) and stored over "titanocene". Argon, nitrogen, and hydrogen gases were passed over MnO on vermiculite and activated molecular sieves.[29] Carbon monoxide (Matheson) and ^{13}CO (MRC-Mound) were used directly from the cylinders. Ethylene was purified by three freeze–pump–thaw cycles. Trimethylaluminum (Aldrich) was used as a 2 M solution in toluene. Triethylaluminum (Aldrich) was used as a neat liquid. $\mathrm{Cp^*_2Nb(H)(C_2H_4)}$ (**1**),[15a] $\mathrm{Cp^*_2Nb(H)(CO)}$ (**3**),[30] $\mathrm{Cp^*_2Ta(H)(C_2H_4)}$ (**2**), $\mathrm{Cp^*_2Ta(H)(CO)}$ (**4**), and $\mathrm{Cp^*CpTa(H)(CO)}$ (**5**)[31] were prepared as previously reported.

Many reactions were surveyed by using NMR spectroscopy. Any experiment described herein but not explicitly listed below was carried out in a sealed NMR tube utilizing ~0.3 mL of benzene-d_6 containing TMS or, for variable-temperature experiments, toluene-d_8. Known amounts of the appropriate reagents were added before the tube was sealed at −196 °C.

Nuclear magnetic resonance spectra were recorded on Varian EM390 (90 MHz, ^{1}H), JEOL FX90Q (89.56 MHz, ^{1}H; 22.50 MHz, ^{13}C), JEOL GX400Q (400 MHz, ^{1}H), and Bruker WM500 (500.13 MHz, ^{1}H) spectrometers utilizing standard parameters. Routine infrared spectra were recorded on a Beckman 4240 spectrophotometer using KBr windows and are reported in inverse centimeters. Equilibrium infrared spectroscopic studies employed the Mattson Sirius 100 FTIR with the Starlab UNIX data system. Elemental analyses were determined by the Caltech Analytical Facility and Dornis and Kolbe Microanalytical Laboratory.

Syntheses. Each of the compounds described below was synthesized in quantitative yield according to NMR tube reactions but was isolated in about 50% yield due to the high solubility of the compounds in petroleum ether.

(1) $\mathbf{Cp^*_2Nb(H)(C_2H_4{\cdot}AlMe_3)}$ (6a). $\mathrm{Cp^*_2Nb(H)(C_2H_4)}$ (**1**) (0.503 g, 1.28 mmol) was placed in a round bottom flask. Petroleum ether (~7 mL) was condensed onto the yellow solid at −78 °C C. An $\mathrm{AlMe_3}$/toluene solution (0.64 mL, 1.28 mmol) was added to the cooled solution by syringe. The reaction mixture was allowed to warm to 24 °C with stirring for 15 min. A pale yellow solid was immediately evident. The solution volume was reduced (~3 mL), and the pale yellow solid **6a** was collected by cold (−78 °C) filtration (0.475 g, 1.02 mmol, 79.7%). The solid was refrigerated under $\mathrm{N_2}$. If left at room temperature, the solid slowly becomes orange and loses $\mathrm{AlMe_3}$. ^{1}H NMR ($\mathrm{C_6D_6}$, 34 °C, ~0.1 M): δ 1.61 (s, 30, Cp*), 0.18 (AA′BB′ m, 4, $-CH_2CH_2-$), −0.21 (s, br, 9, $\mathrm{Al(CH_3)_3}$), −2.73 (s, br, 1, NbH). Anal. Calcd for $\mathrm{C_{25}H_{44}AlNb}$: C, 64.64; H, 9.55. Found: C, 64.40; H, 9.52. Mol wt calcd (found, cryoscopic in benzene): 464.52 (376).

(2) $\mathbf{Cp^*_2Nb(H)(C_2H_4{\cdot}AlEt_3)}$ (6b). $\mathrm{Cp^*_2Nb(H)(C_2H_4)}$ (**1**) (0.463 g, 1.18 mmol) was placed in a round-bottom flask with petroleum ether (~4 mL) and $\mathrm{AlEt_3}$ (161 μL, 1.18 mmol). No color change was apparent as all solid went into solution. The solution was cooled to −78 °C, and the pale yellow solid **6b** was collected by filtration (0.416 g, 0.82 mmol, 69.5%). The solid was refrigerated under $\mathrm{N_2}$. ^{1}H NMR ($\mathrm{C_6D_6}$, 34 °C, ~0.1 M): δ 1.57 (s, 30, Cp*), 1.48 (t, J = 7 Hz, 9, $\mathrm{Al(CH_2}CH_3)_3$), 0.48 (q, J = 7 Hz, 6, $\mathrm{Al(}CH_2\mathrm{CH_3)_3}$), 0.11 (AA′BB′ m, 4, $-CH_2CH_2-$), −2.40 (s, br, 1, NbH). Anal. Calcd for $\mathrm{C_{28}H_{50}AlNb}$: C, 66.39; H, 9.95. Found: C, 66.08; H, 9.65.

(3) $\mathbf{Cp^*_2Ta(H)(C_2H_4{\cdot}AlEt_3)}$ (7). $\mathrm{Cp^*_2Ta(H)(C_2H_4)}$ (**2**) (0.20 g, 0.42 mmol) was weighed into a Schlenk vessel and dissolved in petroleum ether (10 mL). The resulting pale yellow solution was treated with $\mathrm{AlEt_3}$ (57 μL, 0.42 mmol) at room temperature and was accompanied by no apparent change in color or solubility. Concentration of the solution to 5 mL followed by slow cooling to −50 °C afforded large, colorless prisms of compound **7** (0.205 g, 0.35 mmol, 82.8%). The crystals were isolated by cannular filtration, dried in vacuo at −78 °C, and stored at −30 °C under $\mathrm{N_2}$. ^{1}H NMR ($\mathrm{C_6D_6}$, 34 °C, ~0.1 M): δ 1.58 (s, 30, Cp*), 1.48 (t, J = 7 Hz, 9, $\mathrm{Al(CH_2}CH_3)_3$), 0.48 (q, J = 7 Hz, 6, $\mathrm{Al(}CH_2\mathrm{CH_3)_3}$), 0.22 (AA′BB′ m, 4, $-CH_2CH_2-$), −1.43 (s, br, 1, TaH).

(4) $\mathbf{Cp^*_2Nb(H)(CO{\cdot}AlMe_3)}$ (8a). $\mathrm{Cp^*_2Nb(H)(CO)}$ (**3**) (0.548 g, 1.40 mmol) was placed in a round-bottom flask. Petroleum

---

[28] Marvich, R. H.; Brintzinger, H. H. *J. Am. Chem. Soc.* **1971**, *93*, 2046–2048.

[29] Brown, T. L.; Dickerhoff, D. W.; Botus, D. A.; Morgan, G. L. *Rev. Sci. Instrum.* **1962**, *22*, 491–492.

ether (~7 mL) was condensed onto the red solid at -78 °C. An $AlMe_3$/toluene solution (0.72 mL, 1.44 mmol) was added to the cooled solution by syringe. The reaction mixture was allowed to warm to 24 °C with stirring for ~1 h. A bright purple solid was immediately evident. The solution volume was reduced (~3 mL), and the bright purple microcrystalline solid **8a** was collected by cold (-78 °C) filtration (0.560 g, 1.20 mmol, 85.7%). The solid was refrigerated under N_2. ^1H NMR (C_6D_6, 34 °C, ~0.1 M): δ 1.66 (s, 30, Cp*), -0.14 (s, 9, $Al(CH_3)_3$), -4.72 (s, br, 1, NbH). Anal. Calcd for $C_{24}H_{40}OAlNb$: C, 62.06; H, 8.68; Al, 5.81. Found: C, 62.11; H, 8.65; Al, 5.90.

(5) $Cp^*_2Nb(H)(CO{\cdot}AlEt_3)$ (8b). $Cp^*_2Nb(H)(CO)$ (**3**) (0.640 g, 1.63 mmol) was placed in a round-bottom flask with petroleum ether (~5 mL) and $AlEt_3$ (230 μL, 1.469 mmol). The red solution immediately became deep blue. The solution volume was reduced (~2 mL), and the deep blue microcrystalline solid **8b** was collected by cold (-78 °C) filtration (0.586 g, 1.16 mmol, 71.2%). The solid was refrigerated under N_2. ^1H NMR (C_6D_6, 34 °C, ~0.1 M): δ 1.70 (s, 30, Cp*), 1.43 (t, J = 8 Hz, 9, $Al(CH_2CH_3)_3$), 0.55 (q, J = 8 Hz, 6, $Al(CH_2CH_3)_3$), -4.77 (s, br, 1, NbH). Anal. Calcd for $C_{27}H_{46}OAlNb$: C, 64.02; H, 9.15; Al, 5.33. Found: C, 64.10; H, 9.18; Al, 5.43. Mol wt calcd (found, cryoscopic in benzene): 506.56 (515).

(6) $Cp^*_2Ta(H)(CO{\cdot}AlEt_3)$ (9). Purple $Cp^*_2Ta(H)(CO)$ (**4**) (0.20 g, 0.42 mmol) was weighed into a Schlenk vessel and dissolved in light petroleum ether (40–60 °C, 10 mL). $AlEt_3$ (57 μL, 0.42 mmol) was added by microsyringe to give a deep royal blue solution. Concentration of the solution to 2 mL followed by slow cooling to -50 °C gave blue crystals of **9** (0.193 g, 0.33 mmol, 78.0%), which were isolated by cannular filtration, dried in vacuo at -78 °C, and stored at -30 °C under N_2. ^1H NMR (C_6D_6, 34 °C, ~0.1 M): δ 1.68 (s, 30, Cp*), 1.50 (t, J = 8 Hz, 9, $Al(CH_2CH_3)_3$), 0.52 (q, J = 8 Hz, 6, $Al(CH_2CH_3)_3$), -3.18 (s, br, 1, TaH).

(7) $Cp^*CpTa(H{\cdot}AlEt_3)(CO)$ (10). This compound was made and treated analogously to **9**, using $Cp^*CpTa(H)(CO)$ (**5**). ^1H NMR (C_6D_6, 34 °C, ~0.1 M): δ 4.47 (s, 5, Cp), 1.65 (s, 15, Cp*), 1.56 (t, J = 8 Hz, 9, $Al(CH_2CH_3)_3$), 0.42 (q, J = 8 Hz, 6, $Al(CH_2CH_3)_3$), -10.2 (s, br, 1, TaH).

(8) $Cp^*_2Nb(R)(CO{\cdot}AlEt_3)$ (R = Me (11), Et (12), CH_2CH_2Ph (13a), C(Me)=C(Me)H (14)). These compounds were not isolated. Each was made by adding 1 equiv of $AlEt_3$ (via syringe) to approximately 25 mg of the appropriate precursor[15,30] in a sealable NMR tube containing toluene-d_8 (~0.3 mL). The green solutions became blue upon addition of triethylaluminum. The NMR tube was evacuated and sealed at -196 °C. The reactions were quantitative by NMR. The transalkylation and subsequent β-H elimination were monitored by ^1H NMR.[17]

(9) $Cp^*_2Nb(Me)(CO{\cdot}AlMe_3)$. $Cp^*_2Nb(Me)(CO)$[30] (0.125 g, 0.31 mmol) was placed in a round-bottom flask. Petroleum ether (~10 mL) and $AlMe_3$/toluene (2.0 M, 0.15 mL, 0.31 mmol) were added as described in procedure 4. The green solution immediately became aqua-blue. A cornflower blue microcrystalline was collected as described in procedure 4 (0.050 g, 0.10 mmol, 33.9%). ^1H NMR (C_6D_6, 34 °C, ~0.1 M): δ 1.47 (s, 30, Cp*), -0.16 (s, 9, $Al(CH_3)_3$), -0.96 (s, 3, $Nb(CH_3)$).

(10) $Cp^*_2Nb(CH_2CH_2Ph)(CO{\cdot}AlMe_3)$ (13b). $Cp^*_2Nb(CH_2CH_2Ph)(CO)$[15a] (0.290 g, 0.58 mmol) was placed in a round-bottom flask with petroleum ether (~3 mL). An $AlMe_3$/toluene solution (2.0 M, 0.30 mL, 0.58 mmol) was added by syringe to the green solution, which had been cooled to -78 °C. The slurry was stirred at -78 °C for ~$^1/_2$ h, becoming blue with time. A cold filtration yielded the robin's egg blue microcrystalline solid **13b** (0.129 g, 0.23 mmol, 51.2%). The solid was refrigerated under N_2. The solid becomes a bright blue oil (see procedure 11) if left for >30 min at room temperature. ^1H NMR (C_6D_6, 34 °C, ~0.1 M): δ 1.51 (s, 30, Cp*), 0.02 (AA′XX′, 2, $NbCH_2CH_2C_6H_5$), 2.76 (AA′XX′, 2, $NbCH_2CH_2C_6H_5$), 7.0–7.6 (m, 5, $NbCH_2CH_2C_6H_5$), -0.17 (s, 9, $Al(CH_3)_3$). Anal. Calcd for $C_{32}H_{48}OAlNb$: C, 67.59; H, 8.51. Found: C, 67.70; H, 8.47.

(11) $Cp^*_2Nb(Me)(CO{\cdot}AlMe_2CH_2CH_2Ph)$ (15). $Cp^*_2Nb(CH_2CH_2Ph)(CO)$[15a] (0.226 g, 0.46 mmol) was placed in a round-bottom flask with toluene (~10 mL). An $AlMe_3$/toluene solution (2.0 M, 0.24 mL, 0.47 mmol) was added by syringe to the green solution, which had been cooled to -78 °C. The solution was allowed to warm to room temperature with stirring. After 14 h the volatiles were removed, leaving an aqua oil. Petroleum ether (~4 mL) was condensed onto the oil. Solid was observed at low temperature, but it became an oil at room temperature. The volatiles were removed, and petroleum ether (~5 mL) was condensed onto the oil again. The robins egg blue microcrystalline solid **15** was isolated by cold filtration (0.111 g, 0.20 mmol, 42.9%). ^1H NMR (C_6D_6, 34 °C, ~0.1 M): δ 1.45 (s, 30, Cp*), 0.81 (AA′XX′, 2, $AlCH_2CH_2C_6H_5$), 3.07 (AA′XX′, 2, $AlCH_2CH_2C_6H_5$), 7.0–7.5 (m, 5, $AlCH_2CH_2C_6H_5$), -0.18 (s, 6, $Al(CH_3)_3$), -0.97 (s, 3, $Nb(CH_3)$). Anal. Calcd for $C_{32}H_{48}OAlNb$: C, 67.59; H, 8.51. Found: C, 67.70; H, 8.47.

(12) Reactions with CO. Each sample was prepared by placing ~25 mg of the compound in a sealable NMR tube with benzene-d_6 containing TMS. Carbon monoxide was admitted to the evacuated tube at -78 °C. The tube was closed, cooled to -196 °C, and sealed. Control experiments with uncomplexed compounds were carried out at the same time and under the same conditions as for the Al complexes.

(13) $Cp^*_2NbH_2(H{\cdot}AlEt_3)$. $Cp^*_2NbH_3$[30] (0.485 g, 1.32 mmol) was placed in a round-bottom flask with petroleum ether (~4 mL) and $AlEt_3$ (0.18 mL, 1.31 mmol). The off-white solid was collected by cold filtration (0.279 g, 0.58 mmol, 43.9%). The solid was refrigerated under N_2. ^1H NMR (C_6D_6, 34 °C, ~0.1 M): δ 1.91 (s, 30, Cp*), 1.17 (t, J = 7 Hz, 9, $Al(CH_2CH_3)_3$), 0.30 (q, J = 7 Hz, 6, $Al(CH_2CH_3)_3$), -1.44 (s, br, 1, NbH_c), -2.13 (d, br, J = 5 Hz, 2, NbH_o). Anal. Calcd for $C_{26}H_{48}OAlNb$: C, 64.98; H, 10.07. Found: C, 64.89; H, 10.18.

Formation Constant Evaluation.[32] (1) $Cp^*_2Nb(H)(C_2H_4)$ (**1**) (0.398 g) was dissolved in benzene in a 2-mL volumetric flask. This solution (0.507 M) and a solution prepared by diluting 0.5 mL of the first solution to 1 mL in a volumetric flask (0.254 M) were used to calibrate the FTIR instrument. The calibration curve, using peak absorbance values for ν(Nb–H) = 1703 cm^{-1}, followed Beer's law. The calibration curve was used to determine the concentration of uncomplexed **1** in 0.20-mL portions of the 0.507 M solution of **1** to which 0.5, 1.0, and 2.0 equiv of $AlEt_3$ had been added and in a 0.20-mL portion of the 0.254 M solution of **1** to which 1 equiv of $AlEt_3$ had been added. Analysis was based on eq 6 and 7, with $K_{Al} = [AlEt_3]_{eq}^2/[(AlEt_3)_2]_{eq}$, $K_{Et} = [\mathbf{6b}]_{eq}/[\mathbf{1}]_{eq}[AlEt_3]_{eq})$, and $K_{Al}K_{Et} = ([\mathbf{6b}]_{eq}[AlEt_3]_{eq})/([\mathbf{1}]_{eq}[(AlEt_3)_2]_{eq})$. The value of $[\mathbf{6b}]_{eq}$ was determined by subtraction of $[\mathbf{1}]_{eq}$ from the known concentration of **1** added. The values of $[AlEt_3]_{eq}$ and $[(AlEt_3)_2]_{eq}$ were determined by using the relationship $[AlEt_3]_T - [\mathbf{6b}]_{eq} = 2[(AlEt_3)_2]_{eq} + [AlEt_3]_{eq}$, assuming $[AlEt_3]_{eq} \approx 0$ to determine $[(AlEt_3)_2]_{eq}$ and then using that value in the equation for K_{Al} ($K_{Al} = 2.22 \times 10^{-5}$ M for $AlEt_3$ in benzene)[33] to determine $[AlEt_3]_{eq}$. In these experiments, $[(AlEt_3)_2]_{eq} \approx 10^{-1}$ M and $[AlEt_3]_{eq} \approx 10^{-3}$ M, so the approximation is reasonable.

(2) A 1.00 M stock solution of $Cp^*_2Nb(H)(CO)$ (**3**) in benzene was used to prepare solutions from 0.025 to 0.100 M for calibration of the FTIR instrument. The calibration curve using ν(CO) = 1863 cm^{-1} did not follow Beer's law over the entire concentration range. (The experiment was repeated once with the same result; peak absorbance and peak integration values both gave the same result.) The actual calibration curve was used to determine the concentration of uncomplexed **3** in solutions of **8a** and in solutions of **3** with 0.4, 0.5, 0.7, and 1.1 equiv of $AlEt_3$ added. Analysis was based on eq 6 and 8 with $K_{Al} = [AlR_3]_{eq}^2/[(AlR_3)_2]_{eq}$, $K_{CO} = [\mathbf{8}]_{eq}/([\mathbf{3}]_{eq}[AlEt_3]_{eq})$, and $K_{Al}K_{CO} = ([\mathbf{8}]_{eq}[AlR_3]_{eq})/([\mathbf{3}]_{eq}\text{-}[(AlR_3)_2]_{eq})$. The value of $[\mathbf{8}]_{eq}$ was determined in a manner analogous to that described above for [**6b**]. The values of $[AlR_3]_{eq}$ and $[(AlR_3)_2]_{eq}$ were determined as above [$K_{Al} = 8.99 \times 10^{-8}$ M for $AlMe_3$ in benzene).[33] In these experiments, $[(AlR_3)_2]_{eq} \approx 10^{-2}$ M and $[AlR_3]_{eq} \approx 10^{-4}$ M.

Structure Determination. Crystals of $Cp^*_2Ta(H)(C_2H_4{\cdot}AlEt_3)$ (**7**) suitable for X-ray diffraction studies were grown from

---

(30) Bell, R. A.; Cohen, S. A.; Doherty, N. M.; Threlkel, R. S.; Bercaw, J. E. *Organometallics* **1986**, *5*, 972–975.

(31) Gibson, V. C.; Bercaw, J. E.; Bruton, W. J.; Sanner, R. D. *Organometallics* **1986**, *5*, 976–979.

(32) (a) Rossotti, F. J. C.; Rossotti, H. *The Determination of Stability Constants*; McGraw-Hill: New York, 1961; Chapter 13. (b) Colthrup, N. B.; Daly, L. H.; Wiberly, S. E. *Introduction to Infrared and Raman Spectroscopy*, 2nd ed.; Academic: New York, 1975.

(33) Smith, M. B. *J. Organomet. Chem.* **1984**, *70*, 13–33.

a concentrated petroleum ether solution by slow cooling to −50 °C. The crystals produced were always relatively large. (In fact, the Nb analogue **6b** generally produced a single, very large crystal under similar conditions.) Crystals of 7 were mounted at low temperature into glass capillaries by using a modified Schlenk vessel and argon flush/vacuum techniques. (The low-temperature handling was required due to the thermal lability of the compound which was described in the body of the paper.) The capillaries were *swiftly* sealed with a microflame and were kept at low temperature until transferred to the diffractometer. The collection of two data sets on different crystals were attempted and failed, but a third data set gave reasonable results. Only those results are reported here.

The crystal used was large (0.5 × 0.7 × 0.9 mm); it was mounted approximately along *a*. The intensity data were collected on a locally modified Syntex $P2_1$ diffractometer equipped with a low-temperature nitrogen gas stream and a graphite monochromater (Mo Kα radiation, $\lambda = 0.7107$ Å). Fifteen reflections were centered, and least-squares refinement of the orientation matrix and unit cell parameters gave the reported cell constants at 220 K. The reflection data from a quadrant of the Ewald sphere ($+h,+k,\pm l$) were collected to $2\theta < 40°$ (2870 reflections with three checks collected after 197 reflections), and an averaged set of 2497 reflections was generated for refinement; the standard deviation of F_o^2 was derived from counting statistics and increased by a term $(0.028F_o^2)^2$; the overall goodness-of-fit upon averaging was 6.07 for all redundant observations (the 127 $0kl$ reflections), and the R(merge) for those reflections with exactly two observations was 0.161 (118 reflections). Of this averaged set, only one reflection (200) with unusual backgrounds was deleted. [The high overall goodness-of-fit and high R(merge) reflect the extent of systematic error in the data, but due to the irregular shape of the crystal we were unable to correct for absorption.] The average intensities were reduced to F_o^2. Atom form factors were taken from ref 34; the form factors for Ta and Al were corrected for anomalous dispersion.

The Patterson map indicated the positions of the Ta and Al atoms, and the subsequent Fourier maps revealed the remainder of the structure. Hydrogen atoms were introduced into the model with idealized geometry; their coordinates and B's were fixed during refinement. The hydrogen atoms on the ethylene unit and the hydride atom were located from difference Fourier maps. Features close (~1.3 Å) to the Ta atom, presumably due to errors from high absorption, made it impossible to successfully refine the coordinate of the hydride atom. However, refinement of the hydrogen atoms on the ethylene unit gave reasonable results. Several cycles of full-matrix least-squares refinement of all non-hydrogen coordinates and anisotropic Gaussian amplitudes, and the four ethylene hydrogen atoms, minimizing $\sum w\Delta^2$ ($w = \sigma_{F^2}^{-2}$, $\Delta = F_o^2 - (F_c/k)^2$), resulted in goodness-of-fit $S = [\sum w\Delta^2/(n - \upsilon)]^{1/2} = 2.75$ ($n = 2496$ reflections and $\upsilon = 283$ parameters), $R_F = \sum ||F_o| - |F_c|| / \sum |F_o| = 0.061$ (2406 reflections, $I > 0$), and $R_F = 0.054$ (2023 reflections, $I > 3\sigma_I$). The greatest shift/error in the final cycle of refinement was less than 0.25 for the four hydrogen atoms and less than 0.05 for all others; the average shift/error was less than 0.05; the final $\Delta\rho$ map showed two peaks of height 3.5 e Å^{-3} symmetrically disposed ~1.3 Å from each tantalum atom, and the remaining peaks had heights no greater than 1.0 e Å^{-3}. All calculations were carried out on a VAX 11/750 with the CRYM crystallographic system.

Acknowledgment. This work was supported by the Director, Office of Energy Research, Office of Basic Energy Sciences, Chemical Sciences Division of the U.S. Department of Energy, under Contract DE-FG03-85ER 13431 and by the National Science Foundation (Grant CHE-83-03735; X-ray facility, Grant CHE-82-19039; Southern California Regional NMR Facility, Grant CHE-79-16324A1). V.C.G. acknowledges support through a NATO Postdoctoral Fellowship administered by the Science and Engineering Research Council, U.K.. C.M. thanks the National Science Foundation for a Predoctoral Fellowship and the Tyler Foundation for a Haagen-Smit Predoctoral Fellowship. We also thank Drs. A. Sylwester and B. Leland, formerly of Caltech, for their assistance with the FTIR experiments and Dr. E. Hoel, of Exxon Corporate Research, for carrying out the CHEMGRAF conformational analysis on the structure.

Registry No. **1**, 95313-60-3; **2**, 100701-96-0; **3**, 95313-69-2; **4**, 100701-95-9; **5**, 100763-04-0; **6a**, 110903-51-0; **66**, 110903-53-2; **7**, 110903-52-1; **8a**, 110934-27-5; **8b**, 110934-29-7; **9**, 110934-28-6; **10**, 110934-30-0; **11**, 110934-35-5; **12**, 110934-33-3; **13a**, 110934-34-4; **13b**, 110934-32-2; **14**, 110934-36-6; **15**, 110934-37-7; $Cp^*_2Nb(Me)(CO\cdot AlMe_3)$, 110934-31-1; $Cp^*_2nBH_2(H\cdot AlEt_3)$, 110903-54-3; $Cp^*_2Nb(Me)(CO)$, 101010-22-4; $Cp^*_2Nb(CH_2CH_2Ph)(CO)$, 95313-70-5; $Cp^*_2Nb(Et)(CO)$, 95313-68-1; $Cp^*_2Nb(CMe{=}CHMe)(CO)$, 96030-31-8; $Cp^*_2NbH_3$, 93558-77-1; $AlMe_3$, 75-24-1; $AlEt_3$, 97-93-8.

Supplementary Material Available: Figure 3, atom labeling scheme, Table III, atom coordinates and thermal parameters, and Table IV, hydrogen atom coordinates (3 pages); a listing of structure factor amplitudes (15 pages). Ordering information is given on any current masthead page.

---

(34) *International Table for X-Ray Crystallography*; Kynoch: Birmingham, England, 1974; Vol. IV, Table 2.2B.